INFLUENCE OF REGIMES OF BURNING HYDROCARBON FUELS ON THE OPTICAL PROPERTIES OF SMOKE AEROSOLS

V.S. Kozlov, M.V. Panchenko, and A.G. Tumakov

Institute of Atmospheric Optics,
Siberian Branch of the Russian Academy of Sciences, Tomsk
Received July 1, 1993

Based on measurements done under laboratory conditions we have studied the variability of the extinction coefficient and angular characteristics of light scattering by smokes from burnt hydrocarbon fuels (wood, turf, coal, oil, and others), depending on the regimes of burning (pyrolysis, combustion), controlled by air humidity variations and heating of smoke particles. Peculiar feature characteristic of many smokes has been revealed that means that the light absorption ability of smokes (soot content) depends on the regime of burning. For example, the smokes produced due to combustion are strongly absorbing, while the pyrolysis smokes are referred to the group of weakly absorbing media. It is also shown in this paper that the smoke generation regimes strongly affect the condensation activity of smoke aerosols.

Processes of smoke generation are of great interest for the problems of atmospheric optics since their study could make it possible to reveal peculiar features of physicochemical composition of smoke particles, and study their activity in the atmospheric processes, and the contribution of smokes to the formation of optical properties of the atmospheric aerosol. In this paper we consider some results of experimental investigations of variations of smoke optical characteristics depending on the regime of a fuel burning, governed by varying relative humidity of air and by heating of the smoke particles. The experiments were carried out under controlled conditions.

Smokes were produced in a big aerosol chamber at the Institute of Atmospheric Optics (volume 1800 m^3) by means of burning natural substances, which usually are the sources of mass fires and are used as fuels, in an electric muffle furnace at a controlled temperature. These substances were wood, coal, turf, oil, and "urban mixture" (60% of wood, 20% of paper, 15% of textile, and 5% of polymers).

Two regimes of burning were considered : 1) pyrolysis – relatively low temperature decomposition without fire at temperature ≈ 500°C and 2) combustion – high–temperature burning (900°C) with fire and with free access of oxygen. Optical characteristics were measured by means of a laser transmissometer[3] and a flow nephelometer[4] equipped with a heater and a moister. The transmissometer measured the extinction coefficient at the wavelength 0.63 μm along a 40–m long path. The nephelometer measured the scattering coefficient $\mu(45°)$ and two cross polarized components $\mu_1(90°)$ and $\mu_2(90°)$ of light scattered at the right angle at the wavelengths 0.44, 0.52, and 0.6 μm. We could vary relative humidity of air flow up to 95% and temperature up to 350°C.

The measurement technique involved the following stages. A piece of fuel with the mass 0.2–1 kg was burnt in a preselected regime. Relative humidity in the chamber was 10–30%, and temperature was 20°C. Initially the smoke raised up to the upper part of the chamber and in 0.5–1 hour uniformly filled all its volume. Then measurements of the optical characteristics and the humidity (hygrograms) and temperature (thermograms) dependences of $\mu(45°)$ were carried out in a homogeneous smoke in 4–5 hours intervals. Mean duration of the measurement cycle was one day.

The measurement results made it possible to investigate the dynamics of variations of the optical characteristics (extinction coefficient ε, angular parameters $\mu(45°)$, linear polarization degree $P(90°) = (\mu_1 - \mu_2) / (\mu_1 + \mu_2)$, and the asymmetry factor of the scattering phase function $A = \mu(45°)/\mu(90°)$. These optical characteristics are given in Table I together with the parameters of humidity (γ) and temperature (η) dependences described below. The polarization degree values are given for three wavelengths 0.44, 0.52, and 0.60 μm, while angular scattering parameters are given only for the wavelength 0.52 μm.

Figure 1 illustrates the variations of the extinction coefficient during the smoke transformation with time. The extinction coefficient for the whole smoke set varied from 0.001 to 0.1 m^{-1}. It was noted in the experiments with the majority of smokes that pyrolysis results in most high turbidity of air [birch (curves *5* and *7*), urban mixture (curves *12* and *14*), and turf (curves *17* and *18*)] compared to other regimes of burning. That shows that the specific yield of optically active aerosol particles, is higher in the pyrolysis regime. Possibly, it can be explained by the low loss of the aerosol producing gases emitted from the burnt substance in the area of burning. However, such a tendency was not observed for such substances as oil (curves *23* and *24*) and coal (curves *19* and *21*). In this case higher turbidity was observed in the combustion regime. Most probable explanation of this is the specific chemical composition of these substances (higher temperature of sublimation and boiling of the components), resulting in lower efficiency of aerosol production at low–temperature pyrolysis.

0235-6880/93/10 733-05 $02.00

TABLE I.

No. of smoke	Substance	Regime of burning	Mass, kg	Time, hour	$\varepsilon \cdot 10^{-3}$, m^{-1}	$\mu(45°) \cdot 10^{-3}$	$P_1(90°)$, %	$P_2(90°)$, %	$P_3(90°)$, %	A	γ	η
1	Pinewood	Pyrolysis	0.50	1.2	88.20	2.49	−23	−20	−14	7.6	0	5.9
				3.5	63.50	2.38	−28	−25	−19	9.2	0	4.8
2			1.00	14.4	52.40	3.32	−26	−22	−20	6.0	0.07	3.8
3		Combustion	0.30	1.5	6.37	0.60	69	70	75	6.9	0.44	2.3
				16.0	3.10	0.21	69	72	67	6.9	0.40	2.2
4		Mixed	0.70	0.4	10.90	1.97	10	16	–	7.0	0.06	3.9
				20.0	–	1.02	4	7	–	8.3	0	4.4
5	Birchwood	Pyrolysis	0.40	18.0	19.90	4.69	−21	−19	−18	8.8	0.03	14.3
				25.0	16.70	1.93	−22	−21	−17	8.8	0.06	9.1
6			0.20	1.5	5.54	1.01	− 2	8	23	7.9	0.18	14.3
				20.0	2.93	0.76	−17	−12	− 2	8.8	0.10	10.0
7		Combustion	0.60	0.6	8.98	0.47	77	80	81	6.2	0.45	1.7
				19.0	5.75	0.27	78	79	82	6.5	0.30	1.6
8			2.00	1.0	19.40	0.86	85	81	81	6.9	0.33	1.5
				21.3	10.30	0.54	78	81	82	6.3	0.23	1.5
9		Mixed	4.00	5.0	61.50	10.30	− 4	− 2	13	9.6	0.05	9.1
10	Pine needle	Pyrolysis	0.30	2.1	49.00	5.71	−24	−24	–	8.0	0.07	14.3
				22.0	16.70	1.54	−25	−24	–	7.7	0.13	6.7
11			0.15	2.6	16.20	2.11	−18	−14	–	8.1	0.11	10.0
				23.2	6.81	0.79	−20	−17	–	8.5	0.12	6.7
12	Urban mixture	Pyrolysis	0.30	1.0	21.70	2.91	− 9	− 7	− 7	7.1	0.29	12.5
				17.0	10.30	1.43	−18	−18	−17	8.3	0.46	8.3
13			0.20	1.0	17.70	2.56	− 9	− 4	–	7.5	0.33	10.0
				19.0	6.40	1.34	−21	−17	–	8.2	0.55	5.9
14		Combustion	0.50	1.2	16.90	0.86	77	76	82	7.2	0.38	1.6
				5.1	17.60	0.77	77	79	81	6.3	0.50	1.6
15	Paper	Pyrolysis	0.20	4.0	14.00	1.80	−24	−23	−20	7.6	0.09	11.1
				22.4	2.06	0.71	−26	−26	−19	8.3	0.10	9.1
16	Cotton	Pyrolysis	0.10	1.1	7.51	1.26	−11	−11	− 5	8.2	0.14	25.0
				17.3	3.47	0.77	−19	−16	− 7	9.8	0.09	12.5
17	Turf	Pyrolysis	0.50	2.1	8.47	2.05	2	12	–	9.2	0.05	100.0
				19.3	4.20	1.80	−19	−15	–	11.1	0.10	25.0
18		Combustion	1.50	1.3	6.19	1.03	49	59	71	6.4	0.36	7.7
				20.5	4.49	0.85	18	25	42	8.9	0.23	4.2
19	Coal	Pyrolysis	0.20	3.1	8.56	1.21	−10	− 9	− 8	6.7	0.02	9.1
				19.2	3.40	0.74	− 9	− 7	− 5	6.9	0	6.7
20		Combustion	1.00	1.1	71.20	5.46	47	54	63	6.9	0	2.1
				4.3	62.50	4.04	49	55	63	6.9	0	2.1
21			0.30	0.5	32.00	2.09	39	44	51	6.9	0	1.9
22	Oil	Combustion	0.25	27	35.4	1.45	69	68	73	5.9	0	1.8
		(500°C)		64	21.00	0.53	65	65	–	6.5	0	1.8
23		(900°C)	0.12	1.1	58.50	2.26	70	72	74	5.3	0	1.5
				5.4	55.90	1.89	67	71	72	6.1	0	1.5
24		Mixed	0.15	4.4	14.90	1.35	22	24	29	6.8	0	3.5
				18.5	7.31	1.27	34	36	36	7.2	0	2.9

Temporal dynamics of ε (see Fig. 1) mainly can be explained by coagulation and sedimentation evolution of the smoke composition. The time constant of the smoke destruction k (the inverse value is equal to the time of ε decrease by e times) changes in the limits from 10^{-2} to $4\cdot10^{-2}$ h^{-1}.

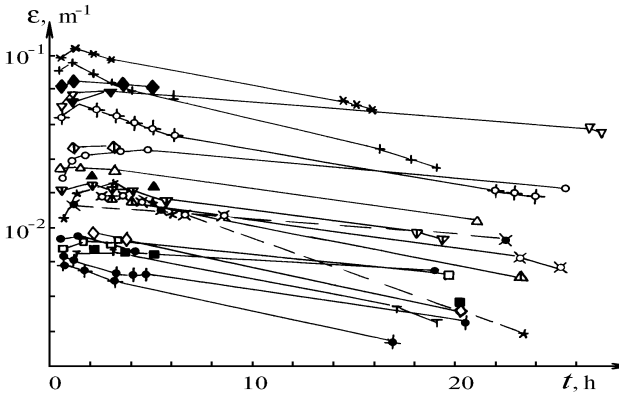

*FIG. 1. Dynamics of the aerosol extinction coefficient. Numbering of smokes is according to that in Table I. Pinewood: pyrolysis (smoke No. 1 by + and No. 2 by *), combustion (No. 3 by ✚, mixed regime (No. 4 by ✖). Birchwood: profiles (No. 5 by ∘ and No. 6 by ✣), combustion (No. 7 by • and No. 8 by ⊖), mixed regime (No. 9 by ◍). Pine needle: pyrolysis (No. 10 by ✣ and No. 11 by ✕); Urban mixture: pyrolysis (No. 12 by Δ and No. 13 by ◭), combustion (No. 14 by ▲). Paper: pyrolysis (No. 15 by ★). Cotton: pyrolysis (No. 16 by T); Turf: pyrolysis (No. 17 by □), combustion (No. 18 by ■); Coal: pyrolysis (No. 19 by ◊), combustion (No. 20 by ◆ and No. 21 by ◈); Oil: combustion (No. 22 by ∇ and No. 23 by ▼), mixed regime (No. 24 by ◥).*

The diagram of the relationship between the directed scattering coefficient μ(45°) at λ = 0.52 μm and the extinction coefficient ε for the investigated smokes is shown in Fig. 2 on double logarithmic scale. This diagram makes it possible to approximately estimate the single scattering albedo Λ. Since $\mu(45°) = \mu_n(45°)\cdot\sigma$, $\sigma = \Lambda\varepsilon$, where μ_n is the normalized scattering phase function, and σ is the scattering coefficient, the following expression holds

$$\log \mu(45°) = \log \varepsilon + \log \mu_n(45°) + \lg \Lambda \ .$$

The points representing the nonabsorbing particles are below the line μ(45°) = ε on $\log \mu_n$, and the absorption (Λ < 1) results in the additional shift by log Λ. The analysis of the calculational data[5,6] for lognormal size–distributions of small absorbing and nonabsorbing particles as well as the results of experimental investigations for the smokes[1,2] show that the values of the normalized scattering phase function values for the angle of 45° vary on the average in the range of $\log \mu_n(45°)$ from −0.8 to −1.

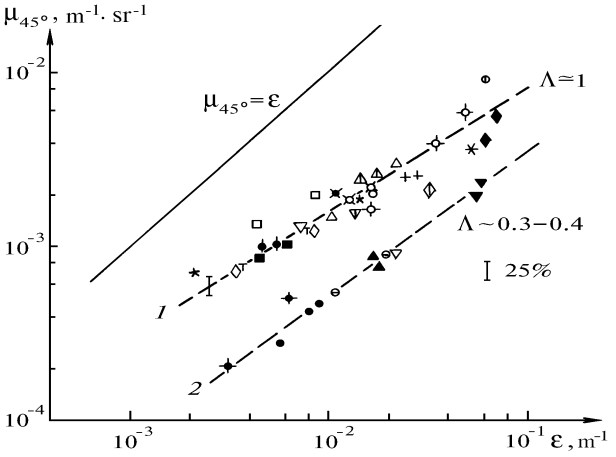

FIG. 2. Diagram of the relationship between directed light scattering coefficient μ(45°) *and extinction coefficient* ε *for the smokes of pyrolysis and combustion. Smoke designation is the same as in Fig. 1.*

As follows from Fig. 2 the smokes produced due to pyrolysis and combustion yield the aerosol with distinct characteristics presented by experimentally obtained curves *1* and *2*. The straight line (*1*) is shifted relative to the axis line μ(45°) = ε by the amount corresponding to difference between the absorbing and nonabsorbing particles. Therefore the data grouped around line (*1*) represent the smokes of weakly absorbing particles, Λ ≃ 1. At the same time smokes represented by data grouped around curve (*2*) obviously have significant absorption (Λ ≃ 0.3–0.4) proportional to the shift, log Λ, of this curve relative to curve (*1*). As is seen, practically all smokes produced in the regime of pyrolysis are weakly absorbing while the strongly absorbing smokes are produced due to combustion. It is natural that strong absorption should be related to in the combustion regime with its great intensity of production of heavy hydrocarbons and soot in the smoke aerosol under the conditions of high–temperature burning of a fuel. Let us note that the smokes of burning turf (18) and coal (20, 21) are not related to the group of strongly absorbing particles on the diagram. May be this is caused by a peculiar feature of the chemical composition of these fuels.

Thus revealed difference between weakly and strongly absorbing smokes, depending on the regime of burning, well agrees with the results of the classification of smokes according to the connection between the angular characteristics of scattering, $P(90°)$ and A (Fig. 3). Use of such a diagram for estimating the microstructure and optical characteristics of particles as well as for classification of smokes by their optical properties has been shown to be useful in Ref. 7. The pyrolysis and combustion smokes are distinctly divided into two specific groups on the diagram. The first group of data in the diagram represents the smokes of pinewood, birchwood, urban mixture, and oil (curves *3*, *7*, *14*, *22*, and *23*) produced in the regime of combustion. These smokes are characterized by high values of the polarization degree $P > 0.6$ and relatively small asymmetry of the scattering phase function A, and by weak spectral dependence of P (Table I) and low variations of the optical parameters at smoke aging (arrows in Fig. 3 indicate the change of the smoke optical state during measurements). The whole set of optical parameters shows that smokes of the first group are mainly composed of small strongly

absorbing particles (soot) whose optical properties only slightly vary with time. The second group is the weakly absorbing smokes (II). It occupies the wide range of possible values of the polarization degree $-0.3 \le P \le 0.6$. It contains all smokes of pyrolysis, some smokes of combustion (turf, coal), and the smokes produced in mixed regimes. The subgroup of coarse dispersed smokes of pyrolysis $P(90°) \lesssim 0$ can readily be separated out of the second group of smokes. It is characterized by a weak spectral dependence of the polarization degree, $P(\lambda)$. Temporal variability of the coarse dispersed smokes is revealed in the increase of the negative polarization accompanied either by an increase or a decrease of the scattering asymmetry (11, 12, 13, 15, 16, 1, 2, 5, 10). Strong spectral dependence $P(\lambda)$ and variability of optical parameters when aging is characteristic of the subgroup of finely dispersed weakly absorbing smokes. The calculational data presented in Fig. 3 for the single mode lognormal size–distributions of particles with the refractive index $n = 1.5$, the absorption index $\kappa = 0.1$, and the variances of the distribution $s^2 = 0.2$ and 0.5 show that these tendencies of the temporal transformations can be explained by an increase of the mean effective size of the smoke particles (the growth of particles results in a decrease of the polarization degree).

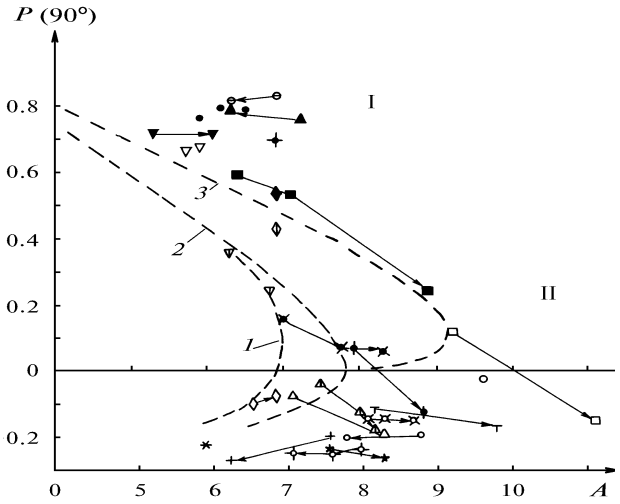

FIG. 3. Diagram of the relationship between linear polarization degree P(90°) and the asymmetry parameter of the scattering phase function A for temporal transformation of smokes. Smoke designation is the same as in Fig. 1. Calculation data: n = 1.50; 1) $s^2 = 0.5$, $\kappa = 0$; 2) $s^2 = 0.2$, $\kappa = 0$; 3) $s^2 = 0.2$, $\kappa = 0.1$.

The determining influence of the regime of the smoke production on the absorption properties of smokes is also confirmed by the results of measuring the smoke thermograms. Characteristic temperature dependences of $\mu(45°)$ at temperatures up to 350°C are presented in Fig. 4*a*. They show that the thermograms of the combustion and pyrolysis smokes are essentially different. The smokes produced in the combustion regime (3, 7, 8, 14, 22, 23) are characterized by the thermograms of the first type with a relatively slow decrease (less than two times, on the average) of $\mu(45°)$ quantitatively described by the parameter of burning out of particles when heating $\eta = \mu(25°C)/\mu(350°C)$. At the same time a significant (up to ten times) decrease of $\mu(45°)$, i.e., thermogram of the second type, is observed for the smokes of pyrolysis. Since the rate of $\mu(45°)$ fall off is indicative of the portion of volatile species in the smoke aerosol substance, it is evident that the smokes of pyrolysis consist of particles with a high content of light hydrocarbons (resinous and other substances) which are essentially volatile. In their turn, the smokes of combustion are composed of particles with a significant portion of heavy nonvolatile hydrocarbons that are inert at heating. According to the kinetic theory of soot production,[8] this fact shows that oxidation of gaseous products of burning in the smokes of combustion is more efficient and, correspondingly, the content of soot in them is higher.

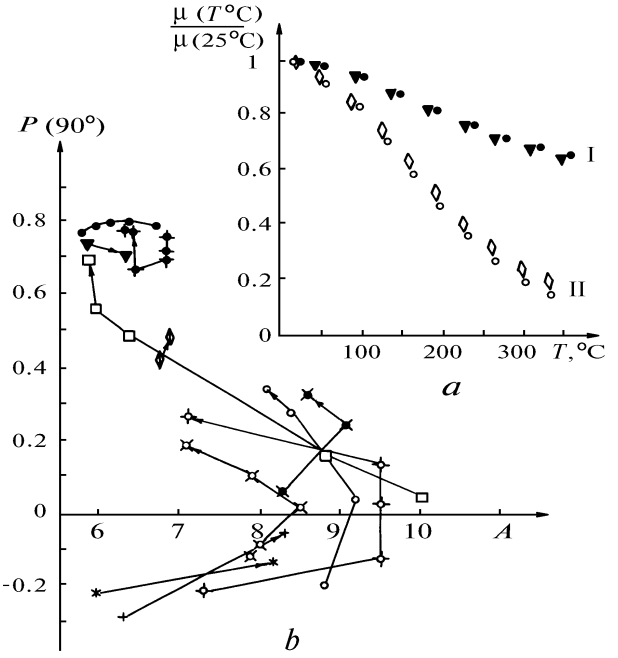

FIG. 4. Variability of the angular scattering characteristics of the smokes of pyrolysis and combustion when heating smoke particles: a) characteristic thermograms of smokes; b) diagram of the relationship between polarization degree and asymmetry parameter of the scattering phase function. Smoke designation is the same as in Fig. 1.

Let us note a particular behavior of "nontypical" smokes of combustion that are not included in the strongly absorbing group. They are coal smoke (20, 21) that also is characterized by low rate of burning out of substance and the turf smoke (18) that has, on the opposite, high rate of burning out. It is reasonable to connect these peculiarities with the specific features of chemical compositions of these fuels and, accordingly, with the difference in the oxidation stages they reach in the regimes of burning considered.

It should be noted, based on measurement data on angular characteristics of light scattering obtained when heating the smokes, that weak variations of A and $P(90°)$ are typical for strongly absorbing smokes of combustion (Fig. 4*b*), that means that these smokes contain particles of strongly burnt out substance (high content of soot). At the same time significant variations of light scattering parameters are characteristic of smokes of pyrolysis. These variations correspond to the decrease of the average particle size: an increasing $P(90°)$ from negative to positive polarizations and decreasing scattering asymmetry. In the case of coarse disperse smokes the curve of increasing degree of polarization crosses the temperature axis (smokes 5, 10, 11, 12, 15, 16, and 19) at a point between 200 to 250°C.

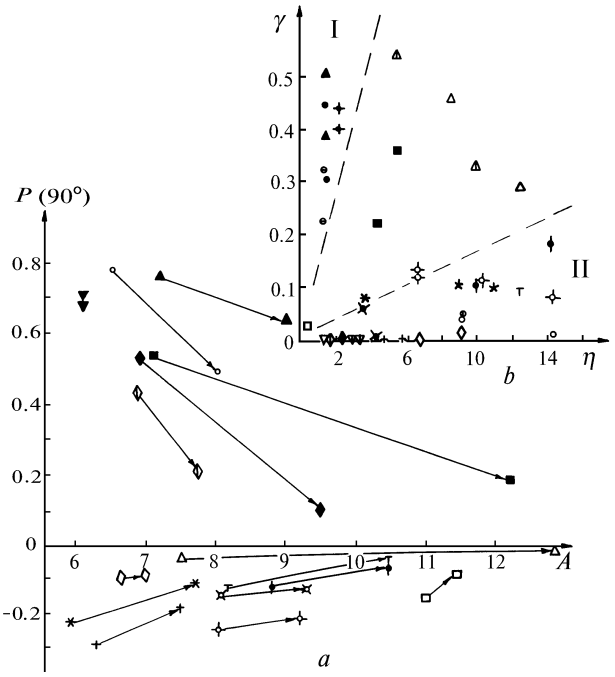

FIG. 5. Variability of the angular scattering characteristics when moistening smoke particles (a) and the relationship between the condensation activity parameter γ with the parameter burning out particles when heating the smoke (b). Smoke numbering is the same as in Fig. 1.

The analysis of data on moistening smoke aerosols shows that the increase of relative humidity up to 95% is usually accompanied by the change of the scattering parameters $P(90°)$ and A (Fig. 5*a*). This circumstance is indicative of the condensation variability of the microphysical characteristics of smokes. The tendency of such transformations (shown by arrows in the figure), i.e., the decrease of the polarization values with simultaneously increasing a symmetry parameter, shows that the condensation watering of particles takes place that usually results in their growth and decrease of optical constants of aerosol substance.

Recording of hygrograms of $\mu(45°)$ makes it possible to estimate the parameter of condensation activity of smokes γ (Table I) according to Kasten and Hänel formula $\mu(r) = \mu(r = 0)(1 - r)^{-\gamma}$, where r is the relative humidity of air. The relationship between γ and the rate of burning out of fuel substance η is shown in Fig. 5*b*. One can select the smokes of oil (22, 23, and 24) and coal (19, 20, and 21) which have low burning out rate and hydroscopic activity independently on the regime of burning. They represented in the figure by points at its lower left part. Possibly, for oil smoke it is connected with the fact that the particles are nonhygroscopic. This well agrees with the data on weak variability of the angular parameters of light scattering by this smoke (Fig. 5*a*). In their turn, the smokes of urban mixture (12, 13, and 14) are characterized by a high condensation activity $\gamma \sim 0.35$–0.4 in both regimes of burning.

The following tendencies are typical for interrelated variations of γ and η of other smokes, depending on the regime of smoke production. The smokes of pyrolysis (1, 2, 4, 5, 6, 10, 11, 15, 16, and 17) are strongly burnt out ($\eta \sim 10$), and characterized by low ($\gamma \sim 0$–0.1) condensation variability of the scattering coefficient. These smokes are presented in the figure by a separate area (II) on the diagram. The smokes of combustion (3, 7, 8, and 18) are weakly burnt out ($\eta \le 2$) and have higher condensation activity ($\gamma > 0.1$), and $\gamma = 0.4$–0.5 can reach the values. The area (I) represents in the figure the smokes of combustion and it is different from the area (II) representing the certainly smokes of pyrolysis. This result clearly demonstrates qualitative differences in the microstructure of smokes produced under different conditions.The peculiarities of the connection between the rate of burning out and the condensation activity revealed for the considered smokes can be a basis for the development of techniques for identification of the prehistory (origin) of smoke aerosols. Let us note in addition that the mixed regimes of smoke production are characteristic of natural processes of burning. Evidently, the optical properties of smokes are determined by the superposition and the difference between the contribution, coming from smokes of pyrolysis and combustion. The considered smokes of mixed regimes (Table I) are close in their optical properties to the smokes of pyrolysis. It should be supposed that low condensation activity of smokes of pyrolysis is due to the "passivation" of the surface of smoke particles by weakly soluble resinous and other substances present in the smoke gases of pyrolysis that are actively burnt out in the aerosol phase. Relatively high condensation activity of the strongly absorbing (highly burnt out) smokes of combustion can be explained by the action of the well–known microcapillary mechanism of the assimilation of moisture by smoke particles which are the products of an intense coagulation of microparticles.

The results of investigation allow us to reveal the peculiarities of the influence of regime of burning hydrocarbon fuels on the characteristics of qualitative composition of smoke particles (strong absorption, inner structure). The particles composition determines, finally, the optical properties of smoke aerosol and the tendencies of its transformation in condensation processes.

REFERENCES

1. V.V. Veretennikov and V.S. Kozlov, *Investigations of Atmospheric Aerosol by the Laser Sounding Techniques* (Nauka, Novosibirsk, 1979), pp. 186–202.
2. V.V. Lukshin and A.A. Isakov, Izv. Akad. Nauk SSSR, Fiz. Atmos. Okeana **24**, No. 3, 250–261 (198).
3. G.M. Vilochkin, V.S. Kozlov, V.G. Oshlakov, and V.V. Pol'kin, in: *Abstracts of Reports at the Seventh All–Union Symposium on the Laser Radiation Propagation in the Atmosphere,* Tomsk (1983), pp. 269–272.
4. M.V. Panchenko, A.G. Tumakov, and S.A. Terpugova, *Instrumentation for Remote Sensing of the Atmosphere* (Tomsk Affiliate of the Siberian Branch of the Academy of Sciences of the USSR, Tomsk, 1987), pp. 40–46.
5. V.S. Kozlov and V.Ya. Fadeev, *Tables of Optical Characteristics of Light Scattering by Fine Dispersed Aerosol with Lognormal Size Distribution,* Preprint No. 31, Institute of Atmospheric Optics, Siberian Branch of the Academy of Sciences of the USSR, Tomsk (1981), 66 pp.
6. E.G. Yanovitskii and V.O. Dumanskii, *Tables on Light Scattering by Polydispersed System of Spherical Particles* (Naukova Dumka, Kiev, 1972).
7. V.S. Kozlov and V.Ya. Fadeev, *Abstracts of Papers at the Second All–Union Conference on Atmospheric Optics,* Tomsk (1980), Part 2, pp. 38–41.
8. P.A. Tesner, *Carbon Production from Hydrocarbons of the Gas Phase* (Khimia, Moscow, 1972).